Assessing stability and performance of fluorine-doped tin oxide electrodes for peroxide formation in carbonate-based electrolytes

Fernanda da Costa Romeiro [a,b], Marcelo Ornaghi Orlandi [a], Guido Mul [b], Kasper Wenderich [*,b], Bastian Mei [*,b,c]

[a] São Paulo State University (UNESP), Institute of Chemistry, Araraquara. 55 Prof. Francisco Degni St, Araraquara, SP 14800-060, Brazil
[b] MESA+ Institute, Photocatalytic Synthesis Group, University of Twente, P. O. Box 217, 7500 AE Enschede, The Netherlands
[c] Industrial Chemistry, Ruhr-University Bochum, Universitätststr. 150, 44801 Bochum, Germany

ARTICLE INFO

ABSTRACT

Hydrogen peroxide (H_2O_2) is a valuable chemical currently produced industrially on a large scale by the anthraquinone process. Recently, carbonate and/or bicarbonate-induced selective water oxidation to hydrogen peroxide has been suggested as an environmentally friendly alternative. In this manuscript, we discuss the effect of electrolyte concentration and type of cation in selective water oxidation using carbonate-based electrolytes (i. e., Na_2CO_3, K_2CO_3 and Cs_2CO_3) on fluorine-doped tin oxide (FTO) electrodes. Based on the experimental observations and a techno-economic evaluation we reveal that K_2CO_3 is preferred over Na_2CO_3 and Cs_2CO_3 electrolytes. Using 5 M K_2CO_3 a Faradaic efficiency of > 60 % was achieved at industrially relevant current densities of 100 mA cm^{-2}. Although for 5 M Cs_2CO_3 electrolytes lower potentials are required at otherwise similar process conditions, a lower efficiency for hydrogen peroxide formation has been observed which is assigned to higher degradation in Cs-containing electrolyte, rendering the use of potassium-based electrolytes more efficient. Independent of the electrolyte used, the electrodes suffered from stability issues as revealed by increasing concentrations of tin in the electrolyte and electrode failure after polarization for several hours. Overall, this work provides detailed knowledge about the impact of electrolyte concentration and type of cation and reveals the importance of appropriate cell design and process operation for meaningful hydrogen peroxide synthesis by mediated-anodic water oxidation.

1. Introduction

Hydrogen peroxide (H_2O_2) is a potential energy carrier and environmentally benign oxidant that decomposes to water and oxygen only [1,2]. This "green" chemical compound is widely used in several applications such as paper and textile bleaching [2,3], water treatment [4], sanitization [5] and chemical synthesis [6], with a growing market value that has been evaluated to be $6.6 billion by 2026 [7]. Industrially, H_2O_2 is mostly produced by the anthraquinone autoxidation process, which is energy-demanding, involves the use of harmful organic compounds and requires expensive metal catalysts and downstream processing including distillation steps to generate large volumes of concentrated H_2O_2 [8–10]. For this reason, the development of sustainable and simple approaches for H_2O_2 production is urgently needed. Electrosynthesis is a cost-effective and environmentally friendly approach and the reductive formation of H_2O_2 by selective oxygen reduction has been frequently studied. Recently also anodic H_2O_2 formation via the two-electron water oxidation reaction (2e$^-$ WOR) (2 H_2O $\rightleftharpoons$ H_2O_2 + 2H$^+$ + 2e$^-$, E° = 1.76 V vs RHE [11]) has been considered as an attractive process. A selective WOR process is particularly attractive due to the possible coupling with other cathodic reactions, such as the hydrogen evolution reaction (HER), or the hydrogen peroxide formation by oxygen reduction with the opportunity to develop a paired electrolysis cell with 200 % efficiency. Therefore, the overall cost efficiency of the whole electrolysis to generate value-added products at the anode and cathode can be enhanced and can thus fit industrial economic demands.

Besides the growing interest in electrocatalyst development [12], also the influence of bicarbonate (HCO_3^-) and/or carbonate (CO_3^{2-}) anions on the WOR selectivity towards H_2O_2 has been studied [12–16]. For example, Mavrikis et al. found that when CO_3^{2-} was the prevalent anion in the electrolyte mixture, an increase of 26.5 % in the faradaic

efficiency (FE) for H_2O_2 production was observed, compared to HCO_3^- anions [17]. Pangotra et al. [13] showed that anodic H_2O_2 production, using a commercial boron-doped diamond (BDD) electrode, increased from 16.4 mmol L^{-1} in $KHCO_3$ to a maximum of 70 mmol L^{-1}, with a peak FE of 57 % in K_2CO_3 solutions. Similarly, Wenderich et al. [18] observed Faradaic efficiencies of up to 31.7 % at 2.90 V vs RHE and corresponding H_2O_2 production rate of 3.93 μmol min^{-1} cm^{-2} in 1 M Na_2CO_3 electrolyte. These studies demonstrate that carbonate electrolytes present undeniably beneficial effects for H_2O_2 production. Recently even highly concentrated potassium carbonate (5 M K_2CO_3) electrolytes were used in combination with FTO electrodes and an outstanding selectivity for H_2O_2 was reported [17,19]. Interestingly, Cs-based electrolytes have been rarely used despite their high solubility and their reported positive influence on the oxygen evolution reaction [16,20–22]. Thus, the role of cations on the selectivity of WOR to H_2O_2 should be further exploited. Finally, it is important to note that the hydrogen peroxide quantification in carbonate and bicarbonate-based electrolytes is challenging. According to Schanz et al. [14] the parallel formation of oxidant species, aside from H_2O_2, such as peroxymonocarbonate, can influence the quantification methods of H_2O_2 [14]. As such identifying the ideal electrolyte is still important.

Fluorine-doped tin oxide (FTO) is frequently used as support electrode material [15,23–25] and accordingly its stability in different electrolytes and within a wide potential window has been assessed [25, 26]. According to Geiger et al. [25], FTO is stable in the potential window -0.34 $V_{RHE} < E < 2.7$ V_{RHE} with no indication of dissolution in 0.1 M H_2SO_4 electrolyte, while dissolution occurs at higher potentials. However, the stability of FTO electrodes in alkaline carbonate solutions and specifically the impact of cations has not been addressed in detail. Therefore, a consistent investigation on the selectivity and stability of FTO in the context of selective water oxidation is needed.

In this work, we perform parallel analysis of the influence of (i) carbonate-based electrolyte concentration, and (ii) alkali metal cations on the H_2O_2 formation. Additionally (iii) the stability of the FTO anodes is assessed and with the generated data set (iv) the techno-economic feasibility is evaluated. Combining electrochemical measurements, thorough hydrogen peroxide quantification, inductively coupled plasma−optical emission spectrometry (ICP-OES) and scanning electron microscopy (SEM) it is shown that potassium containing electrolytes are preferred for the anodic synthesis of hydrogen peroxide. Overall, a higher FE for 2 M K_2CO_3 compared to 2 M Na_2CO_3 and 2 M Cs_2CO_3 electrolytes is shown, suggesting lower H_2O_2 degradation. In addition, a direct relationship between the ionic concentration of CO_3^{2-} and enhanced anodic H_2O_2 formation is observed, leading to a maximum FE of > 60 % when operated in 5 M K_2CO_3 at 100 mA cm^{-2}. Yet the stability of FTO electrodes was beneficial in Cs_2CO_3 electrolytes under anodic polarization, particularly when compared to Na_2CO_3 electrolytes. Considering this discrepancy in activity-stability relation we finally reveal through a techno-economic evaluation the financial benefits of K_2CO_3 over Na_2CO_3 and Cs_2CO_3.

2. Experimental

Fluorine-doped tin oxide (FTO) electrodes were purchased from Sigma Aldrich ($L \times W \times D$ 300 mm × 300 mm × 2.2 mm, surface resistivity ~13 Ω/sq). A custom-made Teflon divided cell has been used for all electrochemical experiments (see the schematic representation in Figure S1a-b). A three-electrode configuration was used, with FTO (1.22 cm^2) acting as the working electrode, a Pt mesh as the counter electrode and a Hg/HgO electrode (1 M NaOH) as the reference electrode. Na_2CO_3, K_2CO_3 and Cs_2CO_3 electrolytes were used as anolyte and H_2SO_4 was used in the catholyte compartment (see details in supporting information A Nafion exchange membrane (Perfluorinated membrane, Sigma-Aldrich, thickness 0.007 in) was used to separate the anolyte and catholyte compartments. A potentiostat (Biologic VMP3 Multichannel Potentiostat) was used for the electrochemical measurements. Cyclic voltammetry (CV) was obtained at a scan rate of 20 mV s^{-1}. For experiments regarding the selective oxidation of water to H_2O_2, chronopotentiometry measurements were performed in different periods of time (10 min and 30 min), current densities (5, 12.5, 25, 50 and 100 mA cm^{-2}) and also fixed charge (C) measurements until 10 C was reached. Potentials were converted to the reversible hydrogen electrode (RHE) scale using the Nernst equation: $E_{(RHE)} = E_{(Hg/HgO)} + 0.059*pH + E^0_{(Hg/HgO)}$, with $E^0_{(Hg/HgO)} = 0.098$ V, and the V_{RHE} was assumed to be equal to V_{cell}. The ohmic drop correction was performed through the ZIR technique (at 85 % compensation). The resistance and pH measured for the different electrolytes are summarized in Table S1. The experiments were performed at room temperature. The experimental information of H_2O_2 quantification, including calibration curves (Figure S2) and characterization techniques used are described in detail in the Supporting Information. Techno-economic evaluations were carried out using a modified version of the models used in previous work done within our group [1, 18]. Here, the levelized cost of hydrogen peroxide (LCHP) is calculated. An explanation on the techno-economic evaluation is provided in the Supporting Information.

3. Results and discussion

3.1. Electrolyte effect in anodic H2O2 production

In this work, the $2e^-$ WOR performance of FTO electrodes has been investigated using Na_2CO_3, K_2CO_3 and Cs_2CO_3 as electrolyte and the Faraday efficiency has been evaluated in a large current density range (5 - 100 mA cm^{-2}, Figure S3) and using different durations.

Benchmark experiments were performed in 1 M electrolyte solutions and the selectivity of FTO towards H_2O_2 synthesis was examined by measuring the obtained H_2O_2 concentration and consequently determining the corresponding faradaic efficiencies ($FE_{H2O2} = 20.5$ % in 1 M K_2CO_3, $FE_{H2O2} = 17.1$ % in 1 M Na_2CO_3 and $FE_{H2O2} = 14.9$ % in 1 M Cs_2CO_3 at 12.5 mA/cm^2). Recently, Gill et al. [16] observed a similar trend for the $2e^-$ WOR to H_2O_2: an increasing order of $Cs^+ < Na^+ < K^+$ was observed for the partial H_2O_2 current density and the FE using a combination of $MHCO_3/M_2CO_3$ (M = cation) electrolytes. This suggests that the use of K_2CO_3 over Na_2CO_3 and Cs_2CO_3 electrolytes is preferred for H_2O_2 evolution. Considering the good performance in 1 M electrolytes, the time-dependent production and FE of H_2O_2 in higher electrolyte concentration (2 M K_2CO_3) was further evaluated in 30 min and 10 min, as shown in Figure S4a-b. The best H_2O_2 production rate (0.36 mmol min^{-1} cm^{-2} at 100 mA cm^{-2}) and the highest FE (30.1 % at 30 mA cm^{-2}) were observed in 10 min of chronopotentiometry in 2 M K_2CO_3 rather than 30 min. Even though a lower concentration of H_2O_2 is observed after 10 min compared to 30 min operation (Table S2), the longer duration experiments reveal that the selectivity towards hydrogen peroxide is continuously decreasing, likely caused by parasitic subsequent reactions, i.e., decomposition. To verify the effect of longer chronopotentiometry times on the FE for H_2O_2 in the 2 M K_2CO_3 applying a current density of 25 mA cm^{-2}, we observe a decay in the FE from FE = 29.1 % in 10 min to a FE = 6.7 % after 60 min (Figure S5). Clearly H_2O_2 consumption by decomposition will cause the overall FE to decrease, yet also H_2O_2 accumulation in the electrolyte during longer experiments might lead to a decay in process selectivity [19]. The use of continuous flow electrochemical cells is advised to study long term performance of the process.

Furthermore, comparison of the influence of cations was performed during shorter constant current experiments of 10 min. First, cyclic voltammetry (CV) scans in three different 2 M electrolytes (Figure S6) were performed. Slightly higher current densities were observed for the Cs_2CO_3 compared to the K_2CO_3 and Na_2CO_3, which indicates a higher electrochemical activity for WOR. However, the highest production rate was observed for 2 M K_2CO_3, see Figure S7a. The highest FE was observed for 2 M K_2CO_3 electrolytes (FE = 30.1 %) for experiments performed at 25 mA cm^{-2}, as depicted in Figure S7b. The FE in Na_2CO_3

(FE = 25.4 %) and Cs_2CO_3 (26.8 %) are clearly lower. It is however important to note that the overall trend changed and Cs-containing carbonate electrolytes are superior to Na_2CO_3 when higher electrolyte concentrations are used.

For all three electrolytes, higher current densities resulted in a lower FE, and only minor differences were observed for the different cations, as shown in Figure S7b. This optimum selectivity at 25 mA cm^{-2} can be related to the best correlation between a high production of H_2O_2 and its oxidation/self-decomposition at high pH regimes. This is for example evident when a high current density of 100 mA cm^{-2} is applied: even though a higher H_2O_2 concentration and production rate are measured, the lower FE observed indicates a combined effect of enhanced oxygen evolution and electrolytic H_2O_2 decomposition [13,21].
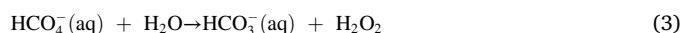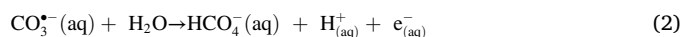
Following recent literature [19] also short duration chronopotentiometry measurements were performed, in which a maximum of 10 C was passed through the system enabling proper data quantification despite the low amounts of H_2O_2 generated. As shown in Fig. 1 for 1 M electrolytes, we observe that the FE for hydrogen peroxide formation using K_2CO_3 electrolyte is higher than in Na_2CO_3 or Cs_2CO_3 for all current densities, reaching a maximum value of 41.6 % when applying 100 mA cm^{-2} (Fig. 1a). When two molar electrolytes are used a FE of 46.9 % was achieved in 2 M K_2CO_3 (at 100 mA cm^{-2}). Overall, the FE in 2 M electrolytes were higher compared to 1 M electrolytes, reinforcing the positive effect of carbonate concentration on the H_2O_2 formation. Despite the higher FE measured at high current density, it is clear that a similar electrolyte-concentration dependent cation trend with K > Na > Cs for 1 M electrolytes and K > Cs ~ Na for 2 M electrolytes is observed. In high concentrations of carbonate solutions, the bulk electrolyte pH is more alkaline (see supporting information, Table S1). As such the change in cation influence is likely associated with the alkalinity of the system that might influence both H_2O_2 production and decomposition. The stability of H_2O_2 in alkaline solutions decreases in the order K >> Na ≈ Cs (Figure S8). Therefore, it appears that H_2O_2 production in Cs-containing electrolytes overrules its decomposition at higher electrolyte concentrations. To obtain a more detailed understanding of the reactivity correlations deriving the pH at the electrode surface under operational conditions might be essential, particularly to resolve the exact electrolyte composition and given that the carbonate/bicarbonate concentration changes with pH. Again, considering that the FE for all electrolytes was observed to be larger for short duration experiments suggests that cell engineering is essential to avoid H_2O_2 decomposition when its production reaches a high concentration after long duration experiments in batch mode operation.

Finally, for potassium and cesium, the influence of cations has been further explored using 5 M electrolytes (see Figures S9, S10 and Fig. 2). For both cations the solubility limit enables the use of highly concentrated electrolytes (K_2CO_3: 1120 g/L at 20 °C and Cs_2CO_3: 2605 g/L at 15 °C) [20]. A maximum FE of 63.1 % using 5 M K_2CO_3 was achieved

and a slightly smaller FE of 59.8 % using Cs_2CO_3 was determined at 100 mA cm^{-2} (Fig. 2c). Moreover, it is worth mentioning that longer duration experiments, i.e., 10 min, a maximum FE of 47.7 % was observed in 5 M K_2CO_3, while a FE peak of 36.7 % was observed in 5 M Cs_2CO_3 (Figure S10a-c). Additionally, 5 M Cs_2CO_3 were not successful for current densities > 50 mA cm^{-2} (see Figure S10b).

All these results suggest that FTO presents an intrinsic selectivity towards the 2e$^-$ WOR, and also that the CO_3^{2-} concentration and the cation can affect the selectivity to H_2O_2. During the carbonate mediated 2e$^-$ WOR, intermediates such as $CO_3^{\bullet-}$, $^{\bullet}OH$ and HCO_4^- can be formed by the application of oxidation potentials on FTO [17,27]. Based on a recent report [19], the validation of the hydrolysis of HCO_4^- anions was confirmed by oxygen exchange between O^{18} isotope-labeled water and carbonate anions, generating abundance of O^{18} in Na_2CO_3 electrolyte after electrolysis.

The FTO electrode offers a stable and conductive catalytic surface to oxidize molecules and form important intermediates for subsequent chemical reactions. In the solution, the presence of carbonate species (HCO_3^- or CO_3^{2-}) depends on the pH of the electrolyte, where CO_3^{2-} species are favored in basic pH and HCO_3^- species in close to neutral chemical environment. In our study, carbonate-based electrolytes were used to indirectly generate peroxide. Therefore, in a first important step, the CO_3^{2-} anions can be oxidized on the positively charged FTO surface. Then, the $CO_3^{\bullet}$ radical can be oxidized to peroxymonocarbonate anions (HCO_4^-). These HCO_4^- can hydrolyze with water to finally generate H_2O_2 and HCO_3^-. The bicarbonate can regenerate the CO_3^{2-} anions to the electrolyte environment, completing the cycle (Eq. (1)-4, Figure S11a) [17,19]. During the water oxidation in carbonate electrolytes, the formation of HCO_4^- is reported to be necessary to further generate H_2O_2 [19].

$$CO_3^{2-}(aq) \rightarrow CO_3^{\bullet-}(aq) + e_{(aq)}^- \tag{1}$$

$$CO_3^{\bullet-}(aq) + H_2O \rightarrow HCO_4^-(aq) + H_{(aq)}^+ + e_{(aq)}^- \tag{2}$$

$$HCO_4^-(aq) + H_2O \rightarrow HCO_3^-(aq) + H_2O_2 \tag{3}$$

$$HCO_3^-(aq) \rightleftharpoons CO_3^{2-}(aq) + H_{(aq)}^+ \tag{4}$$

According to some reports, the cation can affect the electrochemical performances for CO_2 reduction reactions and OER [22,28–31], however it is still unclear how the cation influences the H_2O_2 production. Li et al. [28] suggested that adsorbed Na^+ forms a stronger noncovalent interaction with OH^- through hydrogen bonding than adsorbed K^+, leading to the decrease of interfacial OH^- mobility affecting the OER. Moreover, Garcia et al. [22] elaborated on the positive impact of Cs^+ in OER. Using in situ surface enhanced Raman spectroscopy (SERS) it was suggested that the cation dependence is related to the formation of superoxo OER intermediate. Interestingly, whereas Garcia et al. report
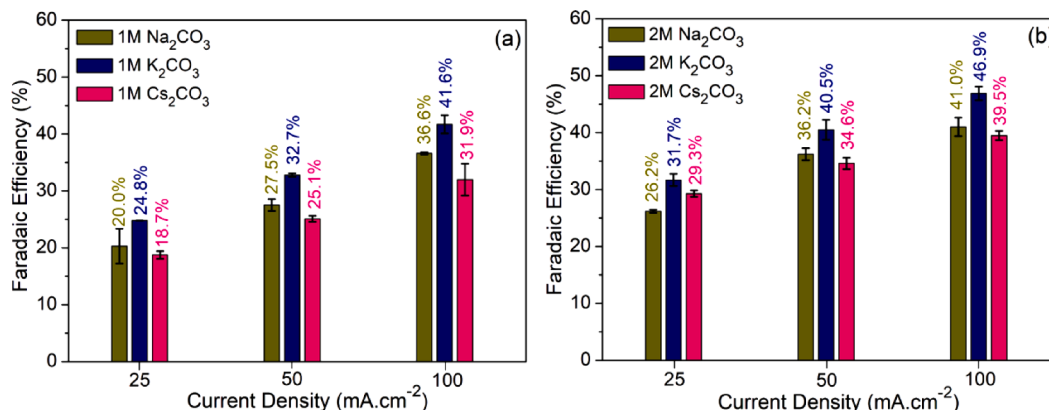

Fig. 1. Faradaic efficiencies for H_2O_2 on FTO at 10 C in (a) 1 M and (b) 2 M Na_2CO_3, K_2CO_3 and Cs_2CO_3 electrolytes.
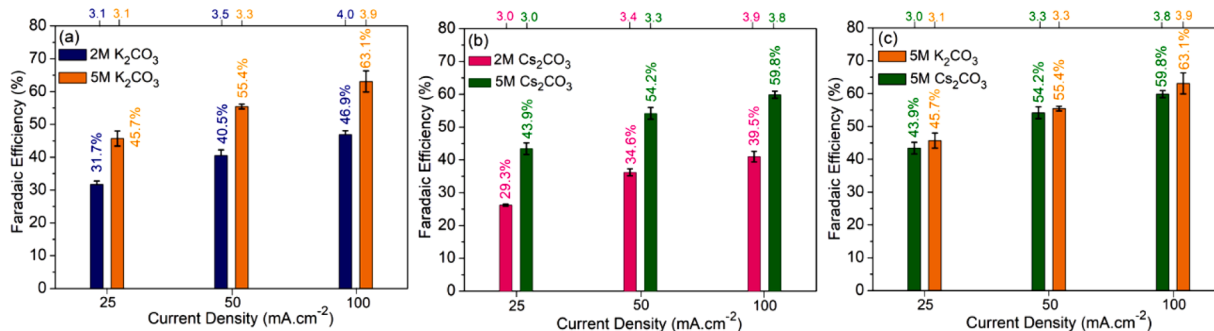
Fig. 2. Faradaic efficiencies of H_2O_2 on FTO after 10 C experiments using (a) 2 M and 5 M K_2CO_3 electrolyte (b) 2 M and 5 M Cs_2CO_3 electrolyte (c) 5 M K_2CO_3 and 5 M Cs_2CO_3 electrolytes.

an increasing trend in OER activity of $Li^+ < K^+ < Na^+ < Cs^+$, a different trend in increasing OER activity was observed by Del Rosario et al. [31]: $Li^+ < Na^+ < Cs^+ < K^+$.

In our experiments, we observed higher FE for H_2O_2 production using K_2CO_3, when compared to Na_2CO_3 and Cs_2CO_3. Thus, a stabilization of intermediate species as reported for OER might indeed also occur during H_2O_2 formation, yet the impact of peroxide decomposition on the net H_2O_2 generation might overrule the positive influence of the larger Cs^+ ions. Interestingly, for short duration experiments (see Fig. 2) at the highest concentrations of Cs^+ and K^+ (5 M), the difference in FE for both cations is significantly smaller compared with similar experiments performed with 2 M electrolytes. Though, more detailed mechanistic understanding is certainly still required, this trend might suggest that Cs^+ indeed have a positive influence on the H_2O_2 formation. Following a similar argumentation as suggested by Li et al. [28] and taking into account that in our study the H_2O_2 is indirectly formed through WOR, the impact of cations might also be explained as follows, taking into account that in our study the H_2O_2 is indirectly formed through WOR. Herein, the alkaline cations can interact through a non-covalent or ionic bond with CO_3^{2-} adsorbed on the FTO surface. In the case of Na^+, these cations form $(H_2O)_x Na^+$-$CO_{3,ad}^{2-}$ clusters that have a direct interaction with the adsorbed CO_3^{2-}. These clusters can be considered as a blockage of active sites (Figure S11b). The K^+ has a minor effect on the WOR, once its larger ionic size can form $(H_2O)_{x-1}K^+$-H_2O—$CO_{3,ad}^{2-}$ clusters, with indirect weaker bonding between solvated water with CO_3^{2-} adsorbed. In this way, in K_2CO_3 electrolyte we can observe higher H_2O_2 formation and higher FE comparing to Na_2CO_3. For Cs-based electrolyte it is discussed in literature that the alkaline cations can influence product formation from CO_2 reduction following $Cs^+ > K^+ > Na^+$ [29,30]. It is suggested by theoretical calculations and experimental data that with increasing cation size, intermediates are stabilized through local electrostatic interactions, [32], including the $CO_2^{\bullet -}$, in-turn leading to lower energy for the C–C coupling step to generate products. Following this analogy, Cs^+ cations (as in Cs_2CO_3 electrolyte) are potentially stabilizing $CO_3^{\bullet}$ radicals enabling the formation of the HCO_4^- intermediates. Yet, the decomposition of H_2O_2 in Cs-based electrolytes prevents even higher efficiencies and as such potassium appears to be the ideal cation when operating in carbonate-based electrolytes. These assumptions need a better fundamental and experimental understanding to uncover the reactions/phenomena in various electrolytes studied herein.

3.2. Electrode stability

To make electrochemical production of H_2O_2 economically interesting, high current densities need to be applied under stable and long term conditions [33,34]. Therefore, long-term stability tests in different concentrations of Na_2CO_3, K_2CO_3 and Cs_2CO_3 electrolytes were performed. It is important to note that during stability evaluation, reaction selectivity has not been explored. The long-term stability can be a big

challenge for oxidation processes due to the high oxidation potentials that can influence the working electrode activity [34]. Detailed description of FTO stability experiments during 30 min and 2 h in 1 M Na_2CO_3, K_2CO_3 and Cs_2CO_3 electrolytes are provided in supporting information from Figures S12 to S17 and Tables S3 and S4. In general, after 2 h applying 25 mA cm^{-2} the degradation of FTO becomes apparent in 1 M Na_2CO_3 electrolyte. After longer chronopotentiometry tests, stability loss of the FTO electrode in 1 M Na_2CO_3, K_2CO_3 and Cs_2CO_3 could be observed, in which irreversible loss of activity in 1 M Na_2CO_3 electrolyte was evidenced after 4 h, while the same was showed after 5 h in 1 M K_2CO_3 and Cs_2CO_3 (Figure S16).

The activity and conductivity loss of FTO in Na_2CO_3 electrolyte can be ascribed to a possible cation replacement between Sn^{4+} in the FTO structure by Na^+ from the electrolyte due to the comparable ionic radius of Na^+ (1.07 Å) and Sn^{4+} (0.69 Å) leading to an instability of the FTO layer, while the ionic radii of K^+ and Cs^+ are 1.38 Å and 1.73 Å, respectively [35,36]. Leaching of tin from the FTO electrode to the electrolyte is already indicated from the Pourbaix diagram, in which at oxidative potentials in alkaline medium (pH > 12.6) formation of soluble tin species (SnO_3^{2-} anions) is indicated [37]. The dissolution of tin from FTO was quantified by ICP-OES complementary analysis (Figure S14). The Sn concentration in the electrolyte is higher when operated in Na_2CO_3 than in K_2CO_3. This increased dissolution is also apparent by the increased porosity of the FTO surface after chronopotentiometry in 1 M Na_2CO_3 and 1 M K_2CO_3 (Figure S13c-f). Particularly, FTO stability has been evaluated in a series of experiments using concentrated electrolytes, i.e., 2 M (Figure S18) and 5 M. The FTO is shown to be more stable in K_2CO_3 and Cs_2CO_3 compared to Na_2CO_3, for which an increase in potential caused by electrode failure is already observed after 3 h when a current density of 50 mA cm^{-2} is applied.

We further evaluated the stability of FTO during electrochemical $2e^-$ WOR performance of FTO electrode in 5 M K_2CO_3 and Cs_2CO_3 electrolytes. The FTO electrode presented excellent stability in 5 M Cs_2CO_3, maintaining a stable potential ranging between 3.3–3.4 V vs RHE for 10 h (Fig. 3a). Nevertheless, pronounced changes of the morphology of the FTO are revealed (Fig. 3c-d), when compared to Fig. 3b and Fig. S13b. This is evidenced by the decrease of FTO particle size (71.2 nm) compared to unused FTO with an average particle size of 96.6 nm as evidenced by the particle size histograms (Figure S19a-b). Moreover, cross-section images reveal a possible electrolyte leakage along the FTO layer until it reaches the silica layer (see Fig. 3d). Nevertheless, elemental mapping of the FTO electrode surface (Figure S20) shows the uniform distribution of Sn, O, F on the glass substrate. Therefore, even though morphology changes after long stability tests in 5 M Cs_2CO_3 electrolyte concentration are observed, the activity of the anodic system remained stable during all experiments indicating the positive effect of the higher concentration of electrolyte on FTO lifetime. On the other hand, electrode failure was already observed after 5 h operation in 5 M K_2CO_3 electrolyte (Figure S21a-b).

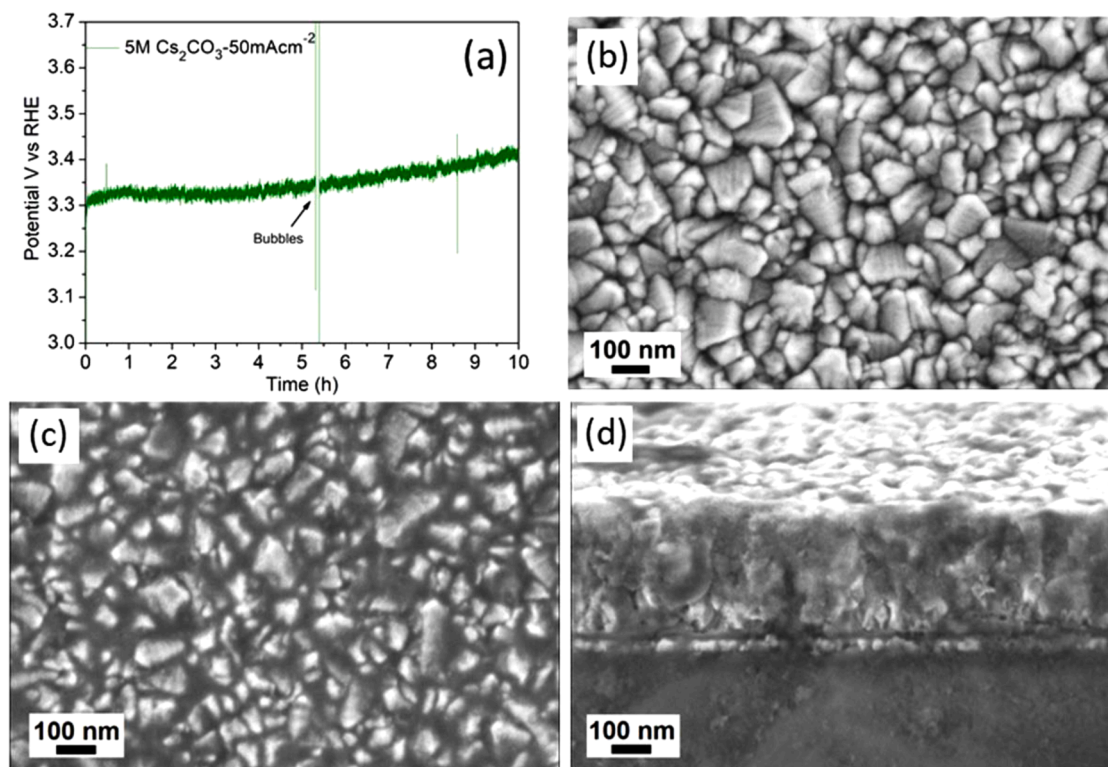It is important to point out that we have used the well-known and

Fig. 3. (a) Long-term chronopotentiometry test (10 h) in 5 M Cs_2CO_3, (b) SEM image of new FTO before chronopotentiometry and (c) SEM image and (d) cross-section images of FTO after 10 h chronopotentiometry in 5 M Cs_2CO_3.

low-cost FTO, as a working electrode to selectively produce H_2O_2. To the best of our knowledge, the electrolytic cation effect on the electrochemical formation of H_2O_2 using carbonate-based electrolytes, and the corresponding FTO electrode stability, are reported here for the first time. The performance parameters, such as FE and production rates, are comparatively lower to some observed in literature, which opens possibilities for further improvements by using other active electrode materials. Such investigations on the selectivity and stability of FTO electrodes in different chemical environments are crucial for future technical electrochemical applications. Moreover, the transfer from batch mode operation to steady-state electrochemical flow rates appears to be crucial to enable simultaneous evaluation of electrolyte governed performance and electrode stability.

3.3. Technoeconomic evaluation

Techno-economic studies are performed based on models designed in earlier work within our group [1,18]). A flowchart depicting the model used is presented in Figure S22. Alterations and the most important calculations in this model are described in detail in the supporting information. Briefly, an industrial plant is assumed where a membrane electrode assembly (MEA) in a flow configuration is used, with H_2O_2 being produced at an FTO anode and H_2 at a Pt cathode. Current for the electrolyzer stack is provided through a photovoltaic (PV) configuration. Because only the financial consequences of using different electrolytes are of interest, we focus on the product evolved at the anode, i.e. hydrogen peroxide. Therefore, the levelized cost of hydrogen peroxide (LCHP) rather than the levelized cost of hydrogen (LCH) is calculated (i. e., the price at which the H_2O_2 needs to be sold to achieve a net present value of 0, see supporting information). It should be noted that in the model no profit for H_2 evolution is assumed [1,18]. Importantly, due to the flow configuration, it is assumed that hardly any degradation of H_2O_2 at the electrode surface takes place; therefore, the FE values reported at a fixed charge of 10 C as reported in Figs. 1 and 2 are used.

Furthermore, the electrolyte is replaced every 7 years, unless noted otherwise.

Calculations of the LCHP for 2 M Na_2CO_3, K_2CO_3 and Cs_2CO_3 are provided in Fig. 4. Here it is evident that the influence of the pricing of the electrolyte is not significant: despite the much higher pricing of the Cs_2CO_3 compared to Na_2CO_3 and K_2CO_3 (a 9-fold higher), the LCHP is in the same order of magnitude. This can be explained due to the low contribution of the anolyte costs compared to the CAPEX excluding the soft balance of systems (0.129 % for K_2CO_3 vs. 0.927 % for Cs_2CO_3). From figure 4a, it becomes clear that at every current density, K_2CO_3 yields the lowest LCHP and is thus financially more attractive than Na_2CO_3 and Cs_2CO_3. Other conclusions which can be drawn, is that the LCHP becomes lower with an increasing current density and concentration. The lowest LCHP ($1.225 kg^{-1}) is found at a current density of 100 mA cm^{-2} at a concentration of 5 M K_2CO_3. This is a promising value, as the price-range reported in 2006 was $0.5–1.2 kg^{-1} [38]. Taking inflation into account, it is very likely that the LCHP determined here can financially compete with industrially produced H_2O_2. Regarding the trends observed, it is likely that higher current densities and concentrations will even further reduce the LCHP.

Interestingly, Gill et al. calculated through a techno-economic evaluation a H_2O_2 price of only $0.46 kg^{-1} when an optimized electrolyte of 0.5 M $KHCO_3$ and 3.5 M K_2CO_3 is used [16]). The discrepancy in costs found in this work can be explained by the financial input used: only the levelized cost of renewable energy is considered in ref [16], whereas the PV costs in our model only makes up a fraction of the CAPEX (10.8 % for 5 M K_2CO_3). Importantly, both in the work of Gill et al. and in this manuscript, the importance of choosing the proper electrolyte is highlighted.

Lastly, we assume in our techno-economic model an electrolyte replacement time of 7 years. This input is regarded from an idealistic perspective. Therefore, we changed the electrolyte replacement time to 1 year in the techno-economic model. Remarkably, we find that the influence of the electrolyte replacement time is negligible. For 5 M
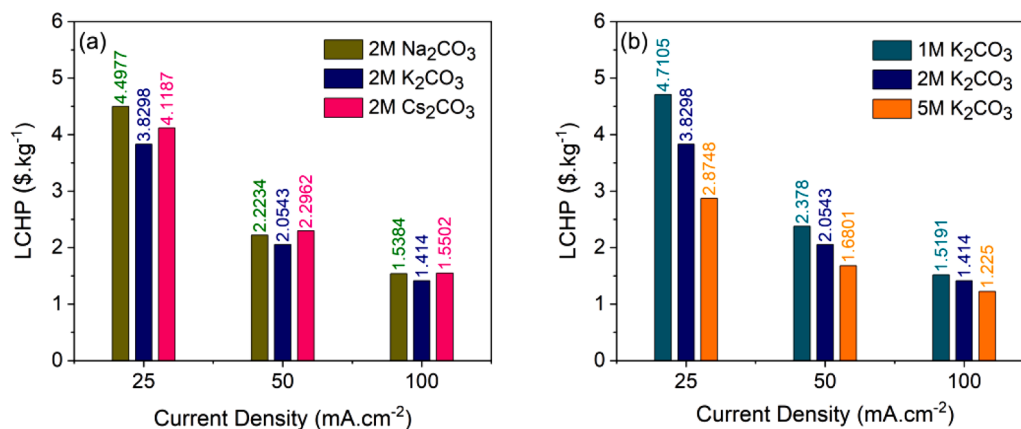
Fig. 4. . Levelized cost of hydrogen peroxide (LCHP) values for (a) 2 M Na_2CO_3, K_2CO_3 and Cs_2CO_3 and (b) 1 M, 2 M and 5 M K_2CO_3 at different current densities.

K_2CO_3, the LCHP is \$1.225 kg^{-1} vs \$1.227 kg^{-1} for electrolyte replacement times of 7 years and 1 year (Figure S23). This means that the LCHP only increases by 0.2 %. Therefore, we conclude that not only experimental results, but also techno-economic analysis clearly indicates that K_2CO_3 is most suitable as an electrolyte for H_2O_2 production, used at a high current density and at a high concentration.

4. Conclusions

In this work, we demonstrate that important parameters including time of experiment, the type of electrolytic cation and the electrolyte concentration influence the FE and production rate of anodically generated H_2O_2 and the stability of the FTO electrodes used in this study. With higher carbonate electrolyte concentrations, higher FE's were attained, where the CO_3^{2-} anions becomes crucial for the successive chemical reactions to H_2O_2 formation. In K_2CO_3 electrolyte, a maximum FE of 63.1 % was achieved at 100 mA cm^{-2} (10 C test) using 5 M K_2CO_3. Thus, potassium-based carbonate electrolyte outperforms carbonate-based electrolytes using Cs or Na. The techno-economic evaluation supports that the use of K_2CO_3 electrolyte is beneficial, and financially more attractive than the use of Na_2CO_3 and Cs_2CO_3. The lowest LCHP (\$1.225 kg^{-1}) was reached at a current density of 100 mA cm^{-2} and at a concentration of 5 M. Our results suggest the importance in choosing the most suitable electrolyte, K_2CO_3, to reach higher FE and long-term stability reactions, which can represent a good perspective for future H_2O_2 industrial applications. FTO represents a low-cost, stable (depending on the electrolyte) and selective electrode for WOR to H_2O_2. As an additional advantage of the anodic H_2O_2 production, this electrochemical process could be coupled to hydrogen production, thereby making the whole water splitting process more valuable to the hydrogen industry.

CRediT authorship contribution statement

Fernanda da Costa Romeiro: Conceptualization, Investigation, Methodology, Validation, Writing – original draft, Writing – review & editing. **Marcelo Ornaghi Orlandi:** Resources, Writing – review & editing, Supervision. **Guido Mul:** Resources, Project administration, Writing – review & editing, Supervision. **Kasper Wenderich:** Investigation, Methodology, Writing – review & editing. **Bastian Mei:** Conceptualization, Investigation, Methodology, Writing – review & editing, Supervision.

Declaration of Competing Interest

The authors declare that they have no known competing financial interests or personal relationships that could have appeared to influence the work reported in this paper.

Supplementary materials

Supplementary material associated with this article can be found, in the online version, at doi:10.1016/j.electacta.2023.143166.

References

[1] K. Wenderich, W. Kwak, A. Grimm, G.J. Kramer, G. Mul, B. Mei, Industrial feasibility of anodic hydrogen peroxide production through photoelectrochemical water splitting: a techno-economic analysis, Sustain. Energy Fuels. 4 (2020) 3143–3156, https://doi.org/10.1039/D0SE00524J.

[2] R. Ciriminna, L. Albanese, F. Meneguzzo, M. Pagliaro, Hydrogen peroxide: a key chemical for today's sustainable development, ChemSusChem 9 (2016) 3374–3381, https://doi.org/10.1002/cssc.201600895.

[3] T. Tzanov, S.A. Costa, G.M. Gübitz, A. Cavaco-Paulo, Hydrogen peroxide generation with immobilized glucose oxidase for textile bleaching, J. Biotechnol. 93 (2002) 87–94, https://doi.org/10.1016/S0168-1656(01)00386-8.

[4] H. Pan, Y. Gao, N. Li, Y. Zhou, Q. Lin, J. Jiang, Recent advances in bicarbonate-activated hydrogen peroxide system for water treatment, Chem. Eng. J. 408 (2021), 127332, https://doi.org/10.1016/j.cej.2020.127332.

[5] J.L. Cadnum, B.S. Pearlmutter, M.F. Haq, A.L. Jencson, C.J. Donskey, Effectiveness and real-world materials compatibility of a novel hydrogen peroxide disinfectant cleaner, Am. J. Infect. Control. 49 (2021) 1572–1574, https://doi.org/10.1016/j.ajic.2021.08.008.

[6] S.P. Teong, X. Li, Y. Zhang, Hydrogen peroxide as an oxidant in biomass-to-chemical processes of industrial interest, Green Chem 21 (2019) 5753–5780, https://doi.org/10.1039/C9GC02445J.

[7] The Worldwide Hydrogen Peroxide Industry is Set to Reach \$6.6 Billion by 2026, (2022). https://www.globenewswire.com/en/news-release/2022/07/07/2475597/28124/en/The-Worldwide-Hydrogen-Peroxide-Industry-is-Set-to-Reach-6-6-Billion-by-2026.html (accessed March 3, 2023).

[8] J.M. Campos-Martin, G. Blanco-Brieva, J.L.G. Fierro, Hydrogen peroxide synthesis: an outlook beyond the Anthraquinone process, Angew. Chemie Int. Ed. 45 (2006) 6962–6984, https://doi.org/10.1002/anie.200503779.

[9] S. Ranganathan, V. Sieber, Recent advances in the direct synthesis of hydrogen peroxide using chemical catalysis—a review, catalysts. 8 (2018). 10.3390/catal8090379.

[10] J. García-Serna, T. Moreno, P. Biasi, M.J. Cocero, J.-P. Mikkola, T.O. Salmi, Engineering in direct synthesis of hydrogen peroxide: targets, reactors and guidelines for operational conditions, Green Chem 16 (2014) 2320–2343, https://doi.org/10.1039/C3GC41600C.

[11] S.C. Perry, D. Pangotra, L. Vieira, L.-I. Csepei, V. Sieber, L. Wang, C. Ponce de León, F.C. Walsh, Electrochemical synthesis of hydrogen peroxide from water and oxygen, Nat. Rev. Chem. 3 (2019) 442–458, https://doi.org/10.1038/s41570-019-0110-6.

[12] J. Baek, Q. Jin, N.S. Johnson, Y. Jiang, R. Ning, A. Mehta, S. Siahrostami, X. Zheng, Discovery of LaAlO3 as an efficient catalyst for two-electron water electrolysis towards hydrogen peroxide, Nat. Commun. 13 (2022) 7256, https://doi.org/10.1038/s41467-022-34884-4.

[13] D. Pangotra, L.-I. Csepei, A. Roth, V. Sieber, L. Vieira, Anodic generation of hydrogen peroxide in continuous flow, Green Chem 24 (2022) 7931–7940, https://doi.org/10.1039/D2GC02575B.

[14] T. Schanz, B.O. Burek, J.Z. Bloh, Fate and reactivity of peroxides formed over BiVO4 anodes in bicarbonate electrolytes, ACS Energy Lett 8 (2023) 1463–1467, https://doi.org/10.1021/acsenergylett.3c00227.

[15] X. Hao, Y. Wei, Y. Honghui, Surface Analysis of Ti/Sb-SnO2/PbO2 electrode after long time electrolysis, Rare Met. Mater. Eng. 44 (2015) 2637–2641, https://doi.org/10.1016/S1875-5372(16)60009-7.

[16] T.M. Gill, L. Vallez, X. Zheng, Enhancing electrochemical water oxidation toward H2O2 via carbonaceous electrolyte engineering, ACS Appl. Energy Mater. 4 (2021) 12429–12435, https://doi.org/10.1021/acsaem.1c02258.

[17] S. Mavrikis, M. Göltz, S. Rosiwal, L. Wang, C. de León, Carbonate-induced electrosynthesis of hydrogen peroxide via two-electron water oxidation, ChemSusChem 15 (2022), e202102137, https://doi.org/10.1002/cssc.202102137.

[18] K. Wenderich, B.A.M. Nieuweweme, G. Mul, B.T. Mei, Selective electrochemical oxidation of H2O to H2O2 using boron-doped diamond: an experimental and techno-economic evaluation, ACS Sustain. Chem. Eng. 9 (2021) 7803–7812, https://doi.org/10.1021/acssuschemeng.1c01244.

[19] L. Fan, X. Bai, C. Xia, X. Zhang, X. Zhao, Y. Xia, Z.-Y. Wu, Y. Lu, Y. Liu, H. Wang, CO2/carbonate-mediated electrochemical water oxidation to hydrogen peroxide, Nat. Commun. 13 (2022) 2668, https://doi.org/10.1038/s41467-022-30251-5.

[20] S. Garg, Q. Xu, A.B. Moss, M. Mirolo, W. Deng, I. Chorkendorff, J. Drnec, B. Seger, How alkali cations affect salt precipitation and CO2 electrolysis performance in membrane electrode assembly electrolyzers, Energy Environ. Sci. 16 (2023) 1631–1643, https://doi.org/10.1039/D2EE03725D.

[21] S. Mavrikis, M. Göltz, S.C. Perry, F. Bogdan, P.K. Leung, S. Rosiwal, L. Wang, C. Ponce de León, Effective hydrogen peroxide production from electrochemical water oxidation, ACS Energy Lett 6 (2021) 2369–2377, https://doi.org/10.1021/acsenergylett.1c00904.

[22] A.C. Garcia, T. Touzalin, C. Nieuwland, N. Perini, M.T.M. Koper, Enhancement of oxygen evolution activity of nickel oxyhydroxide by electrolyte alkali cations, Angew. Chemie Int. Ed. 58 (2019) 12999–13003, https://doi.org/10.1002/anie.201905501.

[23] Q. Gao, H. Jiang, C. Li, Y. Ma, X. Li, Z. Ren, Y. Liu, C. Song, G. Han, Tailoring of textured transparent conductive SnO2:f thin films, J. Alloys Compd. 574 (2013) 427–431, https://doi.org/10.1016/j.jallcom.2013.05.108.

[24] H.-S. Oh, H.N. Nong, P. Strasser, Preparation of Mesoporous Sb-, F-, and In-Doped SnO2 Bulk Powder with High Surface Area for Use as Catalyst Supports in Electrolytic Cells, Adv. Funct. Mater. 25 (2015) 1074–1081, https://doi.org/10.1002/adfm.201401919.

[25] S. Geiger, O. Kasian, A.M. Mingers, K.J.J. Mayrhofer, S. Cherevko, Stability limits of tin-based electrocatalyst supports, Sci. Rep. 7 (2017) 4595, https://doi.org/10.1038/s41598-017-04079-9.

[26] A. Korjenic, K.S. Raja, Electrochemical Stability of Fluorine Doped Tin Oxide (FTO) Coating at Different pH Conditions, J. Electrochem. Soc. 166 (2019) C169, https://doi.org/10.1149/2.0811906jes.

[27] T.M. Gill, L. Vallez, X. Zheng, The role of bicarbonate-based electrolytes in H2O2 production through two-electron water oxidation, ACS Energy Lett 6 (2021) 2854–2862, https://doi.org/10.1021/acsenergylett.1c01264.

[28] G.-F. Li, M. Divinagracia, M.F. Labata, J.D. Ocon, P.-Y.Abel Chuang, Electrolyte-dependent oxygen evolution reactions in alkaline media: electrical double layer and interfacial interactions, ACS Appl. Mater. Interfaces. 11 (2019) 33748–33758, https://doi.org/10.1021/acsami.9b06889.

[29] J. Resasco, L.D. Chen, E. Clark, C. Tsai, C. Hahn, T.F. Jaramillo, K. Chan, A.T. Bell, Promoter effects of Alkali metal Cations on the electrochemical reduction of carbon dioxide, J. Am. Chem. Soc. 139 (2017) 11277–11287, https://doi.org/10.1021/jacs.7b06765.

[30] M.C.O. Monteiro, F. Dattila, B. Hagedoorn, R. García-Muelas, N. López, M.T.M. Koper, Absence of CO2 electroreduction on copper, gold and silver electrodes without metal cations in solution, Nat. Catal. 4 (2021) 654–662, https://doi.org/10.1038/s41929-021-00655-5.

[31] J.A.D. del Rosario, G. Li, M.F.M. Labata, J.D. Ocon, P.-Y.A. Chuang, Unravelling the roles of alkali-metal cations for the enhanced oxygen evolution reaction in alkaline media, Appl. Catal. B Environ. 288 (2021), 119981, https://doi.org/10.1016/j.apcatb.2021.119981.

[32] M.M. Cencer, C. Li, G. Agarwal, R.J. Gomes Neto, C.V. Amanchukwu, R.S. Assary, Interactions of CO2 anion radicals with electrolyte environments from first-principles simulations, ACS Omega 7 (2022) 18131–18138, https://doi.org/10.1021/acsomega.2c01733.

[33] D. Pangotra, A. Roth, V. Sieber, L. Vieira, Electrochemical water oxidation to hydrogen peroxide on bipolar plates, ACS Sustain. Chem. Eng. 11 (2023) 2680–2685, https://doi.org/10.1021/acssuschemeng.2c06314.

[34] F.-Y. Chen, Z.-Y. Wu, Z. Adler, H. Wang, Stability challenges of electrocatalytic oxygen evolution reaction: from mechanistic understanding to reactor design, Joule 5 (2021) 1704–1731, https://doi.org/10.1016/j.joule.2021.05.005.

[35] S. Phadke, R. Mysyk, M. Anouti, Effect of cation (Li+, Na+, K+, Rb+, Cs+) in aqueous electrolyte on the electrochemical redox of Prussian blue analogue (PBA) cathodes, J. Energy Chem. 40 (2020) 31–38, https://doi.org/10.1016/j.jechem.2019.01.025.

[36] I. Ullah, A. Munir, S. Muhammad, S. Ali, N. Khalid, M. Zubair, M. Sirajuddin, S. Z. Hussain, S. Ahmed, Y. Khan, I. Hussain, A. Haider, Influence of W-doping on the optical and electrical properties of SnO2 towards photocatalytic detoxification and electrocatalytic water splitting, J. Alloys Compd. 827 (2020), 154247, https://doi.org/10.1016/j.jallcom.2020.154247.

[37] R. Buckle, S. Roy, The recovery of copper and tin from waste tin stripping solution: part I. Thermodynamic analysis, Sep. Purif. Technol. 62 (2008) 86–96, https://doi.org/10.1016/j.seppur.2007.12.021.

[38] B. Mei, G. Mul, B. Seger, Beyond water splitting: efficiencies of photo-electrochemical devices producing hydrogen and valuable oxidation products, Adv. Sustain. Syst. 1 (2017), 1600035, https://doi.org/10.1002/adsu.201600035.